Soft Matter

RSCPublishing

PAPER
A. van Blaaderen *et al.*
Nucleation of colloidal crystals on
configurable seed structures

2011
C
CHEMISTRY

International Year of
CHEMISTRY
2011

Nucleation of colloidal crystals on configurable seed structures

M. Hermes, E. C. M. Vermolen,† M. E. Leunissen,‡ D. L. J. Vossen,§ P. D. J. van Oostrum, M. Dijkstra and A. van Blaaderen*

Nucleation is an important stage in the growth of crystals. During this stage, the structure and orientation of a crystal are determined. However, short time- and length-scales make nucleation poorly understood. Micrometer-sized colloidal particles form an ideal model system to study nucleation due to more experimentally accessible time- and length-scales and the possibility to manipulate them individually. Here we report experiments and simulations on nucleation in the bulk of a hard-sphere fluid, initiated by seed structures configured using optical tweezers. We find that the defect topology of the critical nucleus determines the crystal morphology. From the growth of the crystals beyond the critical nucleus size, new insights into the role of defects in crystal growth were gained that are incompatible with the assumption of equilibrium growth. These results explain the complex crystal morphologies observed in experiments on hard spheres.

A good understanding of nucleation is of fundamental physical interest but it is also important for many applications. Properties such as orientation, grain size and defect morphology, which determine the mechanical, electrical and optical properties of the material, are determined during nucleation. However, nucleation is a rare event which in molecular systems takes place in a very short time and at small length scales in the bulk of a large system. This makes nucleation very difficult to study. Colloids, with their experimentally accessible time and length scales, offer an opportunity to study nucleation on the single particle level. Many studies on nucleation have been performed on colloidal systems of nearly hard spheres.[1–8] However, also in colloidal systems, nucleation at low supersaturation is a rare event that takes place in the bulk of a large system. This is the reason we employ an optical tweezer to construct a seed for the nucleation.[9] The primary aim of this study is to investigate the effects of small two-dimensional seeds brought into the bulk on the nucleation. We investigate whether the nucleation barrier can be lowered by introducing a seed and whether the shape of the barrier can be explained by classical nucleation theory. Additionally, we study the subsequent growth of the crystal nucleus and investigate how the resulting crystal morphology depends on the structure of the seed. Lowering nucleation barriers in the bulk and thereby

increasing the nucleation rate is important for *e.g.* protein crystallization, while gaining control over the self-assembly of colloidal systems is interesting for advanced materials such as photonic crystals.[10]

In general, two types of nucleation can be distinguished: *homogeneous nucleation* in which small crystallites grow in the bulk of an undercooled or supersaturated fluid, and *heterogeneous nucleation* in which crystallites nucleate on a different substance, *e.g.* the surface of another crystal or on a container wall. Homogeneous nucleation can be qualitatively described by CNT: nuclei are formed continually by thermal fluctuations, but most of the time the high surface energy cost of the crystallites is not counterbalanced by the bulk free energy gain and the crystallite melts.[1,11,12] However, if a nucleus is formed that exceeds the critical nucleus size, the bulk free energy term overcomes the surface term and the nucleus grows out. Since the growing nuclei form randomly throughout the sample it is impossible to control homogeneous nucleation. However, crystals grown by heterogeneous nucleation can be precisely controlled by controlling the structure of the nucleating object.[4]

To study heterogeneous nucleation, Cacciuto and Frenkel[13] performed Monte Carlo simulations on finite 2D seed structures in the bulk of a hard-sphere fluid. They observed a pre-critical nucleus, corresponding to a local minimum in the free energy. The pre-critical nucleus consisted of a few layers of crystalline particles attached to the seed structure. The pre-critical nucleus was quite stable for low supersaturation but could already grow out at volume fractions with very low rates of spontaneous nucleation. Cacciuto and Frenkel found good correspondence between the barrier heights predicted by a modified version of CNT and the nucleation rate of their simulations. They studied planar crystalline templates with the structure of the square

Soft Condensed Matter, Debye Institute for NanoMaterials Science, Utrecht University, Princetonplein 1, NL-3584 CC Utrecht, the Netherlands. E-mail: A.vanBlaaderen@uu.nl; Web: http://www.colloid.nl
† Presently: Shell Projects and Technology, Kessler Park 1, NL-2288 GS Rijswijk, the Netherlands.
‡ Presently: FOM Institute AMOLF, Science Park 104, NL-1098 XG Amsterdam, the Netherlands.
§ Presently: Philips Research Laboratories, High Tech Campus 34, NL-5656 AE Eindhoven, the Netherlands.

(100), distorted hexagonal (110) and hexagonal (111) plane of a face centered cubic (FCC) structure and concluded that the hexagonal plane is the most effective in lowering the nucleation barrier. They also suggest that the number of seed particles can be drastically reduced by choosing a larger particle spacing that is also commensurate with the crystal without affecting the effectiveness of the seed. In experiments, this would allow for larger seeds using the same number of seed particles. We investigate in experiments and simulations whether we can indeed use seeds with a large spacing to reduce the number of particles in the seed structure. Additionally, we compute the nucleation barriers for such seeds using computer simulations and we compare them with a modified version of CNT.

The free energy difference between FCC and hexagonal close-packed (HCP) crystals of hard spheres at coexistence is very small: 0.0008 $k_B T$ per particle.[14] Because of this small difference, homogeneously nucleated hard-sphere crystals have a random hexagonal close-packed (RHCP) structure.[5,15,16] The internal structure of the critical nuclei has been studied in experiments[1] and computer simulations[12,17] both finding FCC as well as HCP stacked layers for hard-spheres, although a more careful analysis showed recently that the critical nucleus contains significantly more FCC than HCP stacked particles.[24] On the other hand, O'Malley and Snook showed using molecular dynamics (MD) simulations that the structure of crystallites is more complex and consists predominantly of multiple twinned crystal domains that are formed by blocks of FCC crystals bound by stacking faults.[18] We investigate whether the stacking of the crystal can be influenced by choosing a square seed, which is only compatible with FCC, or a hexagonal seed, which is compatible with both FCC and (R)HCP.

I.   Methods

The particles that formed the bulk of the experimental dispersion were PMMA particles which were completely dyed with 1,1′-dioctadecyl-3,3,3′,3′-tetramethylindocarbocyanide perchlorate (DiIC) and sterically stabilized with poly(12-hydroxystearic acid) (PHS). The PHS was not locked to the particles. These host particles were $\sigma = 0.93$ μm in diameter. The seed particles were made from polystyrene cores with a diameter of 0.99 μm onto which a thin 50 nm silica shell was grown as described in ref. 19. Subsequently, the silica shell was coated with 3-(trimethoxysilyl) propyl methacrylate and the PMMA-PHSA steric stabiliser.[9] The final diameter of the seed particles was $\sigma_s = 1.1$ μm. The solvent matched the index of refraction of the PMMA host particles at 1064 nm (the infrared wavelength of the trapping laser) and consisted of a mixture of cyclohexyl bromide (CHB) and cis-decalin. We verified that the bulk fluid particles were unaffected by the presence of an empty optical trap, as the density profile remained structureless. The interactions between the particles were tuned to be nearly hard-sphere-like by saturating the solvent with the salt tetrabutylammonium bromide (TBAB). The combined confocal microscopy and optical tweezers setup used in this paper is described in ref. 9. The dielectrophoretic compression was obtained by a 'slit-like' geometry as described in ref. 20. The cell was approximately 15 mm by 8 mm by 70 μm and the slit was approximately 0.3 mm wide.

Event driven MD simulations were performed on 100 000 hard spheres with diameter σ and mass m. The particles in the seed were fixed to their positions and the collisions with these particles were treated as if the fixed particles had infinite mass. A cubic box with periodic boundaries was used. To study whether the particles were part of the nucleus, we calculated the Q_6 bond
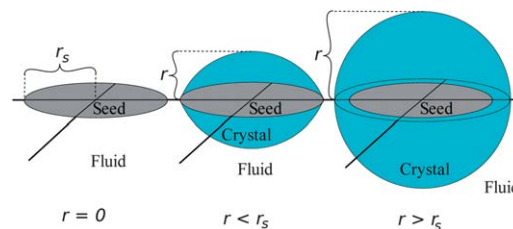

Fig. 1 Schematic picture of CNT on a template. The seed structure is assumed to be circular with radius r_s. The crystal is assumed to have the shape of two spherical caps for $r < r_s$ and of one whole sphere for $r > r_s$.
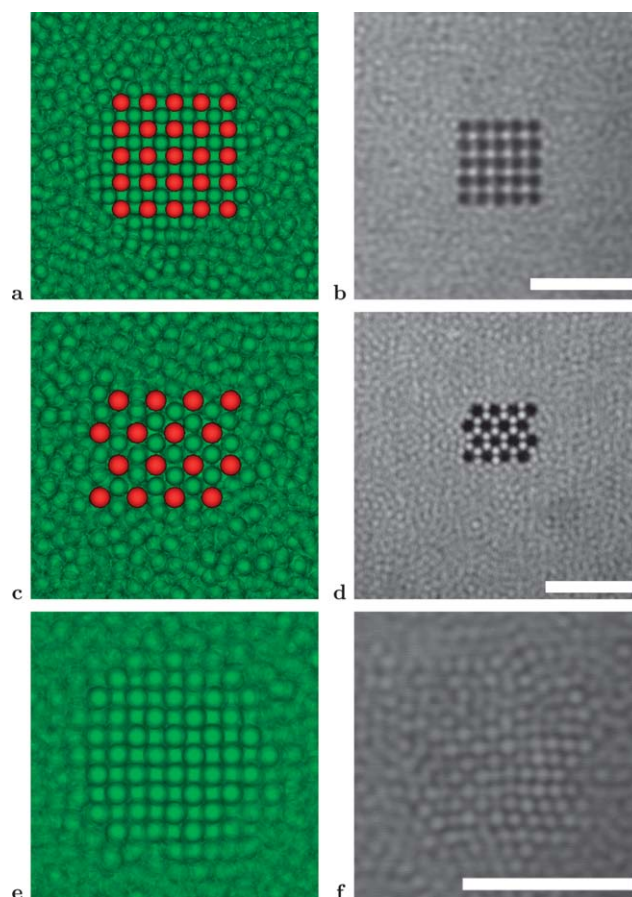

Fig. 2 Structure of the fluid particles around the seeds. The top four images (a,b,c and d) show the particles around the seed are at a volume fraction below coexistence ($\eta \approx 0.49$). Shown at the left (a, c and e) are time-averaged snapshots from an MD simulation and at the right (b, d and f) are time-averaged confocal images where the undyed seed particles are visible as black spots. Images (a,b,e and f) show square seeds of 25 particles with a spacing of approximately 1.91 diameters, (c and d) show hexagonal seeds of 16 particles with a spacing of approximately 1.56 diameters (of the free particles). In (e and f) are the pre-critical nuclei of approximately 120 particles one layer above the square seed structure at volume fraction $\eta = 0.51$. The scale bars are 10 μm.

correlation order parameters.[21–23] A distance criterion of 1.4 diameters was used to define bonds. We used 0.6 for the cutoff of the bond order and 7 as the minimum number of correlated bonds of a crystalline particle. Two crystalline particles with a bond correlation of 0.95 or higher were considered as part of the same crystalline domain.

We have followed the scheme of Cacciuto and Frenkel to adapt CNT to a seed structure.[13] The only modification is that we have placed our seed in the middle of the crystallite since this yields a lower free energy and corresponds to the observations in our simulations and experiments. Thus the Gibbs free energy to form a crystalline cluster reads:

$$\Delta G = \gamma_{\mathrm{fs}} S - \Delta\mu \rho_{\mathrm{s}} V + E_{\mathrm{si}} \qquad (1)$$

where S is the surface area of the nucleus, V is the volume of the nucleus, γ_{fs} is the interfacial tension between the fluid and the solid, $\Delta\mu > 0$ is the chemical potential difference between fluid and the solid, ρ_{s} is the density of the solid and E_{si} is the interaction energy between the fluid-solid interface and the fixed seed particles. In our case the surface area of the nucleus is given by:

$$S = \begin{cases} 2\pi(r^2 + r_s^2) & r < r_s \\ 4\pi r^2 & r > r_s \end{cases}, \qquad (2)$$

and the volume is given by:

$$V = \begin{cases} \dfrac{\pi}{3} r(3r_s^2 + r^2) & r < r_s \\ \dfrac{4}{3}\pi r^3 & r > r_s \end{cases}, \qquad (3)$$

where r_s is the radius of the seed and r is the height of the nucleus measured from the center of the seed. Here we assume that the cluster on the seed structure has the shape of a spherical cap of radius r_s and height r, which becomes spherical when $r > r_s$. We will ignore the seed interface interactions and set E_{si} to zero. To compare with the experiments and simulations we chose r_s such that the circular seed area matched the area of the seed structure used in experiments and simulations.

II. Results

The experiments were started at a volume fraction $\eta = \pi\sigma^3 N/6V = 0.30$, where N is the number of particles and V the volume. The colloids were slowly compressed in the slit, with on average a total time between $\eta = 0.30$ and 0.50 of 180 min. The simulations were performed at a fixed particle volume fraction. The volume fraction was chosen such that the free energy barrier to nucleate on the seed was several $k_B T$ to ensure that the pre-critical nucleus had time to equilibrate before it grew out.

The particles in the seed were not touching, and the spacing was chosen such that exactly one particle could fit in between neighboring seed particles as can be seen in Fig. 2 and Fig. 4. The larger spacing was required in the experiments to avoid overlap of neighboring optical traps. The particle spacings were chosen
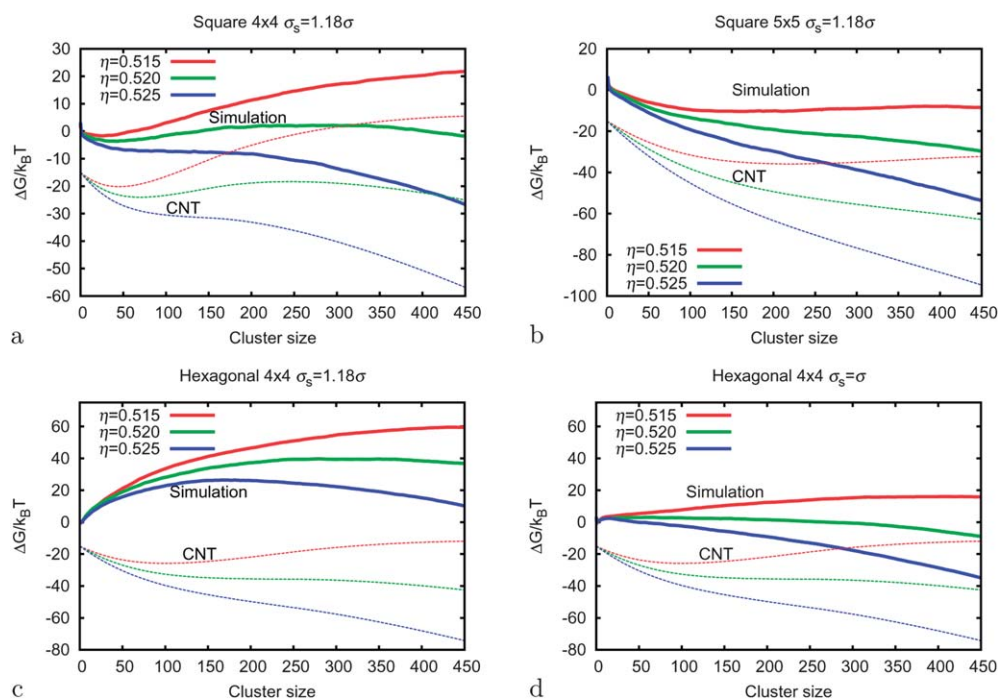

Fig. 3 The Gibbs free-energy barrier as a function of cluster size, *i.e.* the number of particles in the crystalline cluster, on preset 2D seeds. The solid lines are obtained with *NPT* umbrella sampling Monte Carlo simulations. The dashed lines are obtained from modified CNT with a surface tension $\beta\sigma^2\gamma_{fs} = 0.66$. The CNT barriers are offset $-15k_BT$ for clarity. The seed particles are of the same size as in the experiment, *i.e.* $\sigma_s = 1.18\sigma$ in (a,b and c), in d they have the same size as the fluid particles. The different colors stand for different volume fractions (as labeled). **a)** The free-energy barrier for a four-by-four square seed with a spacing of 1.56 σ. **b)** The free-energy barrier for a five-by-five square seed with a spacing of 1.56 σ. **c)** The free-energy barrier for a four-by-four hexagonal seed with a spacing of 1.91 σ. **d)** The free-energy barrier for a four-by-four hexagonal seed with a spacing of 1.91 σ. The seed particles are of the same size as the free particles, *i.e.* $\sigma_s = \sigma$.

to match the spacing in a solid at coexistence as closely as possible. The spacing was $\sqrt{2} \cdot 1.1\sigma \approx 1.56\sigma$ for the square seed structures and $\sqrt{3} \cdot 1.1\sigma \approx 1.91\sigma$ for the hexagonal seed structures. The square seeds consisted of 25 particles and the hexagonal seeds consisted of 16 particles. The seed structures in the simulations were equivalent to the ones configured in the experiments. As in the experiments, the seed particles were 1.18 times larger than the host particles, *i.e.* $\sigma_s = 1.18\sigma$.

1. Nucleation

In Fig. 2(a,b,c and d) we show the structure of the fluid around the seed at volume fraction $\eta = 0.49$, slightly below the coexistence density of the fluid. In order to distinguish between the solid and fluid-like particles, the images were averaged over 5–10 frames to emphasize the immobile particles. Fig. 2(a,b,e and f) show that experiments and simulations both yielded a small FCC stacked crystal on the square seed. In Fig. 2(e,f) a slice through the crystallite at a volume fraction slightly above coexistence, one layer above the seed, is shown. The simulation was performed at a volume fraction of $\eta = 0.51$, which lies within the variance of the volume fraction as measured in the experiments. According to CNT, the size of the critical nucleus decreases with increasing density and the probability of growing beyond the critical size increases. At a volume fraction of approximately $\eta = 0.515$ (simulation value) the nucleus grew out beyond the critical size. Bulk nucleation at this density is still extremely unlikely.[17,24] The pre-critical nucleus was found to disappear when the seed particles were released, while a nucleus that was larger than the critical nucleus remained stable even without a seed. A pre-critical nucleus was not found on the hexagonal seeds either in simulations or in experiments (see Fig. 2(e,f)). The hexagonal nucleus did grow out, but at a higher density, which is estimated by simulations to be at a volume fraction of $\eta = 0.535$. Simulations with a hexagonal seed without the larger spacing did show the formation of a pre-critical nucleus. Thus it is indeed possible to use a larger particle spacing to lower the nucleation barrier, however, the square seed does this more efficiently than the hexagonal seed.

To investigate why the pre-critical nuclei were seen on the square seeds, but not on the hexagonal seeds, the nucleation barriers were calculated using the umbrella sampling technique in Monte Carlo *NPT* simulations. In Fig. 3a, the barriers for a four-by-four square nucleus at a spacing of 1.56 σ are plotted. At low density, a local free-energy minimum was found at a finite nucleus size. When the density was increased, the free-energy barrier between this finite nucleus and the crystal phase decreased until it had completely disappeared at a volume fraction between $\eta = 0.520$ and 0.525. For a five-by-five square seed structure, as plotted in Fig. 3b, the barriers are lower and already at a volume fraction of $\eta = 0.515$ the barrier is so low that it can easily be crossed. The critical size and the size of the metastable nucleus obtained from the calculated barriers agrees well with the values obtained from the experiments, the MD simulations and the modified CNT as described in the methods section. However, the precise barrier shape does differ slightly from the CNT barriers. This is most likely caused by the particle spacing and the seed interface interaction which are both not taken into account in the modified CNT. In Fig. 3c, the free-energy barriers for

a four-by-four hexagonal seed with a spacing of 1.91 σ are plotted. The barriers obtained with umbrella sampling MC simulations correspond well with our observations in both experiments and MD simulations. There is no metastable pre-critical nucleus since the metastable free-energy minimum is always at nucleus size zero. However, the modified CNT as described in the methods section,[13] does not match with the other results and predicts barriers that are too low and do have a metastable minimum at finite nucleus size.

To investigate if the larger diameter of the seed particles was the cause of the discrepancy between CNT and the other results on the hexagonal seeds, we also performed simulations with seed particles of the same size as the free fluid particles. For the square seed the free-energy barriers were found to be very similar to the ones with 1.18 times larger seed particles at a slightly higher density (0.005 increase in volume fraction). In case of the hexagonal seeds in Fig. 3d, the barriers were substantially lowered, but still no metastable pre-critical nuclei were observed. Cacciuto and Frenkel[13] have shown that for a seed structure with a spacing of 1.1 σ, such a metastable free-energy minimum does exist. To investigate whether the large particle spacing was the cause of the absence of a pre-critical nucleus in our experiments we also performed simulations with a square seed with a spacing of 2.2 σ. These simulations also yielded barriers without a pre-critical nucleus. From these observations, it can be concluded that the formation of a metastable pre-critical nucleus and the effectiveness of lowering the nucleation barriers of 2D seeds
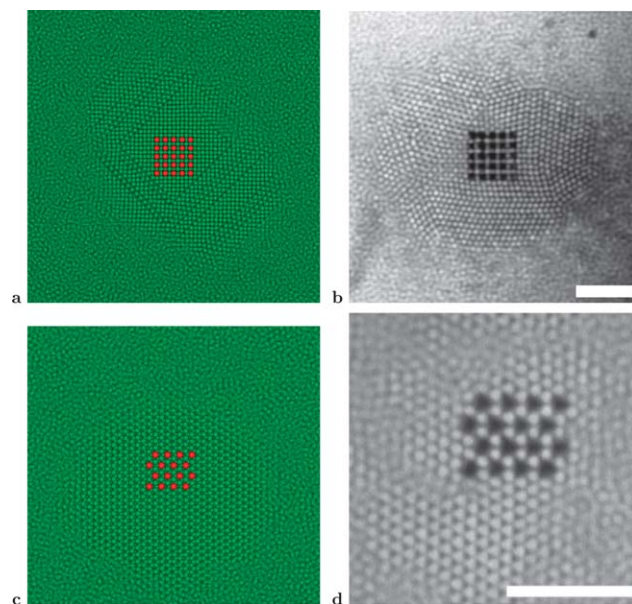

Fig. 4 Crystals growing on 2D square and hexagonal seeds. The crystal on the square seed has grown beyond its critical size at a volume fraction of $\eta = 0.515$ at which the critical size is approximately 400 particles. The crystal on the hexagonal seed has grown beyond its critical size at a volume fraction of $\eta = 0.535$. At the left (a and c) are snapshots from an MD simulation when the crystal was approximately 3×10^4 particles and at the right (b and d) time-averaged confocal images. At the top (a and b) a square seed structure with a spacing of 1.56 σ (of the free particles) and at the bottom (c and d) a hexagonal seed structure with a spacing of approximately 1.91 σ. The scales bars are 10 μm.

depends strongly on the lattice spacing. A new theory or a more advanced version of CNT is needed to fully describe the shape of the nucleation barriers on seeds with a large spacing.

2. Crystal growth

Typical results for crystals that grew beyond the critical nucleus size are shown in Fig. 4. The square seed structure generated an FCC initial nucleus on the seed visible in Fig. 4(a,b). Outside the range of the seed, the crystals were randomly stacked and contained many small domains. There was no sign of bulk crystallization. In the case of the hexagonal seeds, visible in Fig. 4(c,d), most nuclei consisted of a single RHCP domain. In the experiments the first small bulk nuclei are also visible. We observed a tendency to form a cylindrical crystal shape. From these observations, we conclude that the initial stacking of the 3D nucleus that grows on the 2D seed after reaching the critical nucleus size plays an important role in the growth and incorporation of defects in the crystal.

In Fig. 5 we take a closer look at typical defect structures of the growing crystals. In the simulations we used the 3D Q_6 bond correlation order parameter, as described in the methods section, in order to distinguish different domains inside the crystal. It was not possible to obtain reliable 3D coordinates from the experimental images, therefore all major defects were marked by visual inspection (a two dimensional local bond order analysis gave very similar results). Almost all RHCP crystals grown on hexagonal seeds were completely free of grain boundaries and

contained only a few point defects (examples are given in Fig. 5(c,d)). On the other hand, the crystals grown on the square seeds contained many defects. A central FCC-stacked domain originated from the seed and followed the (100) plane induced FCC structure. This central FCC domain is bounded by eight hexagonal planes. When the FCC domain had grown larger than the range of influence of the seed, differently stacked domains formed on some of these hexagonal faces, with twinning defects in between, see *e.g.* Fig. 5(a,b) and Fig. 6. These different domains can not form on the hexagonal seed, since the RHCP nucleus only has hexagonal planes on the bottom and top faces.
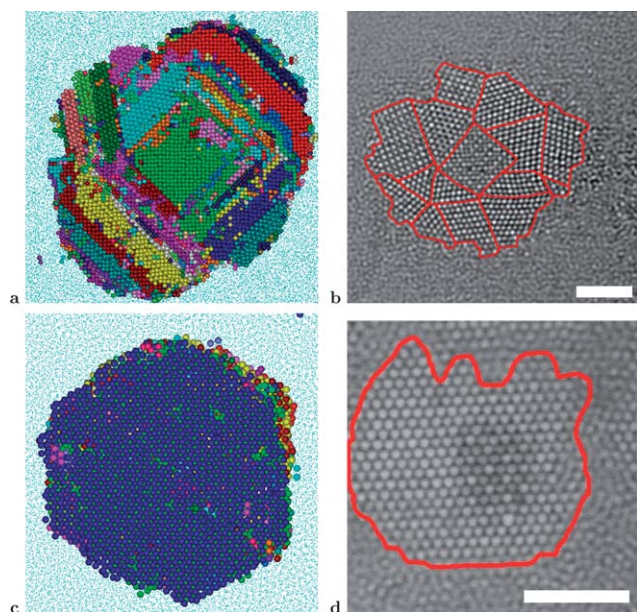

Fig. 5 Defect structures of the growing crystals 2 layers above the seeds. The square (a,b) and hexagonal (c,d) seed simulations on the left and experimental data on the right. In the simulations (a,c) a cluster criterion based on Q_6 was used to determine the crystallinity of the particles. There are 4×10^4 crystalline particles in (a) and 3×10^4 crystalline particles in (c). The crystalline particles are drawn at their normal size and the fluid particles are drawn as dots. A cluster criterion was used to color the different domains. In (b,d) we show, experimental, time-averaged scans to distinguish the fluid from the crystal-like particles. Lines were drawn where irregularities in the crystal were observed. The scale bars are 10 μm.
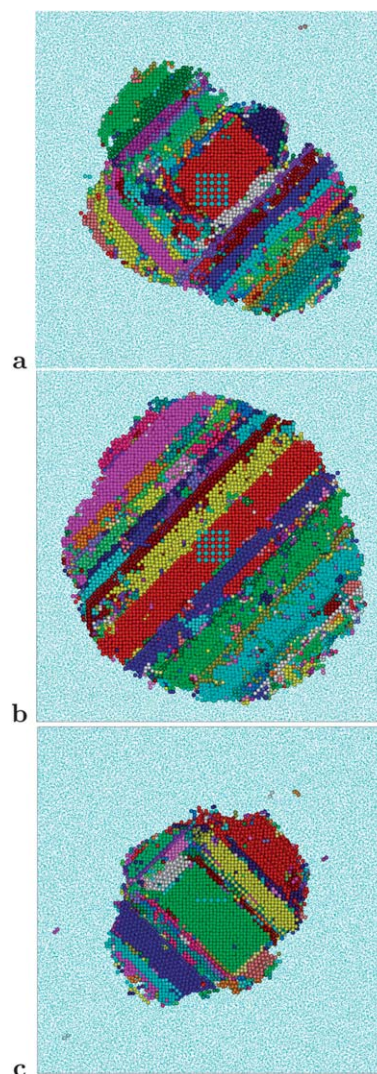

Fig. 6 Snapshots from MD simulations illustrating the different defect structures that were observed on a square seed. The MD simulations were performed with 1×10^5 particles on a square seed of 25 particles and a spacing of 1.56 σ. The fluid particles are drawn as dots. The particles are colored according to the Q_6 criterion described in the methods section. **a)** has a tetrahedral central FCC domain which occurred in 40% percent of our MD simulations. There are 9×10^4 particles in the crystal. **b)** has a central FCC domain that is flat, which was observed in 30% of the simulations. There are 17×10^4 particles in the crystal. **c)** has a central FCC domains that is bounded by six defects. The view is perpendicular to the plane of the seed. There are 5×10^4 particles in the crystal.

To illustrate the broad range of crystal morphologies that was observed for a square seed structure, a few typical structures such as a crystallite with a tetrahedral central FCC domain which occurred in 40% of the MD runs, a flat central FCC domain which occurred in 30% of the MD runs and an FCC domain bound by six stacking faults which occurred in 10% of the MD runs are depicted in Fig. 6. All growing crystals were more or less spherical but had very rough surfaces with deep crevices at the domain boundaries (Fig. 5 and Fig. 6).

III. Conclusion

In conclusion, we have shown that the nucleation barrier can be lowered by introducing a seed structure into the bulk of a supersaturated fluid. However, contrary to what was suggested by Cacciuto and Frenkel[13] it was found that non-touching seed structures are less effective when the particle spacing exceeds a certain threshold. The large spacing of the hexagonal seeds combined with the large size of our seed particles results in barriers that are only slightly lower than the nucleation barriers in the bulk. However, the square seed worked remarkably well and resulted in nucleation at low supersaturation. The modified CNT from Cacciuto and Frenkel[13] works fairly well for our square seeds but fails to describe the barriers of our hexagonal seeds. We have shown that the structure of the initial nuclei that grow further determines not only the shape and orientation but also the domain size and crystal/defect morphology of the resulting crystal. While the square seeds lower the nucleation barrier remarkably well, they result in crystals with significantly more defects than the hexagonal seeds and do not lead to large FCC crystals. Our results on the defect-rich crystals grown on square 2D seeds also strongly indicate that non-equilibrium pathways may become important early on in the crystal growth in many experimental studies on hard-sphere crystal growth.

Acknowledgements

References

1 U. Gasser, E. R. Weeks, A. Schofield, P. N. Pusey and D. A. Weitz, *Science*, 2001, **292**, 258–262.
2 J. L. Harland and W. van Megen, *Phys. Rev. E: Stat. Phys., Plasmas, Fluids, Relat. Interdiscip. Top.*, 1997, **55**, 3054–3067.
3 C. Sinn, A. Heymann, A. Stipp and T. Palberg, *Prog. Colloid Polym. Sci.*, 2001, **118**, 266–275.
4 J. P. Hoogenboom, A. K. van Langen-Suurling, J. Romijn and A. van Blaaderen, *Phys. Rev. Lett.*, 2003, **90**, 138301.
5 J. Zhu, M. Li, R. Rogers, W. Meyer, R. H. Ottewill, S. S. S. Crew, W. B. Russel and P. M. Chaikin, *Nature*, 1997, **387**, 883–885.
6 Z. Cheng, W. B. Russel and P. M. Chaikin, *Nature*, 1999, **401**, 893–895.
7 V. W. A. de Villeneuve, R. P. A. Dullens, D. G. A. L. Aarts, E. Groeneveld, J. H. Scherff, W. K. Kegel and H. N. W. Lekkerkerker, *Science*, 2005, **309**, 1231–1233.
8 E. C. M. Vermolen, A. Kuijk, L. C. Filion, M. Hermes, J. H. J. Thijssen, M. Dijkstra and A. van Blaaderen, *PNAS*, 2009, **106**, 16063–16067.
9 D. Vossen, A. van der Horst, M. Dogterom and A. van Blaaderen, *Rev. Sci. Instrum.*, 2004, **75**, 2960.
10 P. Lodahl, A. van Driel, I. Nikolaev, A. Irman, K. Overgaag, D. Vanmaekelbergh and W. Vos, *Nature*, 2004, **430**, 654–657.
11 S. Auer and D. Frenkel, *Phys. Rev. Lett.*, 2003, **91**, 015703.
12 S. Auer and D. Frenkel, in *Advanced Computer Simulation, Approaches for Soft Matter Sciences I*, Springer, Berlin/Heidelberg, 2005, vol. 173, ch. Numerical Simulations of Crystal Nucleation in Colloids, pp. 149–208.
13 A. Cacciuto and D. Frenkel, *Phys. Rev. E: Stat., Nonlinear, Soft Matter Phys.*, 2005, **72**, 041604.
14 P. G. Bolhuis, D. Frenkel, S. Mau and D. A. Huse, *Nature*, 1997, **388**, 235–236.
15 P. N. Pusey and W. van Megen, *Nature*, 1986, **320**, 340–342.
16 P. N. Pusey, W. van Megen, P. Bartlett, B. J. Ackerson, J. G. Rarity and S. M. Underwood, *Phys. Rev. Lett.*, 1989, **63**, 2753–2756.
17 S. Auer and D. Frenkel, *Nature*, 2001, **409**, 1020–1023.
18 B. O'Malley and I. Snook, *Phys. Rev. Lett.*, 2003, **90**, 085702.
19 C. Graf, D. L. J. Vossen, A. Imhof and A. van Blaaderen, *Langmuir*, 2003, **19**, 6693–6700.
20 M. E. Leunissen and A. van Blaaderen, *J. Chem. Phys.*, 2008, **128**, 164509.
21 P. J. Steinhardt, D. R. Nelson and M. Ronchetti, *Phys. Rev. B*, 1983, **28**, 784–805.
22 J. S. van Duijneveldt and D. Frenkel, *J. Chem. Phys.*, 1992, **96**, 4655–4668.
23 P. R. ten Wolde, M. J. Ruiz-Montero and D. Frenkel, *Phys. Rev. Lett.*, 1995, **75**, 2714–2717.
24 L. Filion, M. Hermes, R. Ni and M. Dijkstra, *J. Chem. Phys.*, 2010, **133**, 244115.